PNAS RESEARCH ARTICLE | CELL BIOLOGY

WNK1 controls endosomal trafficking through TRIM27-dependent regulation of actin assembly

Ji-Ung Jung[a] and Melanie H. Cobb[a,1]

Contributed by Melanie H. Cobb; received January 6, 2023; accepted May 18, 2023; reviewed by J. Silvio Gutkind and Alexander Sorkin

The protein kinase WNK1 (with-no-lysine 1) influences trafficking of ion and small-molecule transporters and other membrane proteins as well as actin polymerization state. We investigated the possibility that actions of WNK1 on both processes are related. Strikingly, we identified the E3 ligase tripartite motif-containing 27 (TRIM27) as a binding partner for WNK1. TRIM27 is involved in fine tuning the WASH (Wiskott–Aldrich syndrome protein and SCAR homologue) regulatory complex which regulates endosomal actin polymerization. Knockdown of WNK1 reduced the formation of the complex between TRIM27 and its deubiquitinating enzyme USP7 (ubiquitin-specific protease 7), resulting in significantly diminished TRIM27 protein. Loss of WNK1 disrupted WASH ubiquitination and endosomal actin polymerization, which are necessary for endosomal trafficking. Sustained receptor tyrosine kinase (RTK) expression has long been recognized as a key oncogenic signal for the development and growth of human malignancies. Depletion of either WNK1 or TRIM27 significantly increased degradation of the epidermal growth factor receptor (EGFR) following ligand stimulation in breast and lung cancer cells. Like the EGFR, the RTK AXL was also affected similarly by WNK1 depletion but not by inhibition of WNK1 kinase activity. This study uncovers a mechanistic connection between WNK1 and the TRIM27-USP7 axis and extends our fundamental knowledge about the endocytic pathway regulating cell surface receptors.

WNK1 | TRIM27 | WASH | endocytosis

WNK1 (with-no-lysine 1) (1) is a serine–threonine protein kinase that participates in signaling cascades controlling cellular responses to osmotic stress (2, 3). The best-known function of the WNK pathway is to phosphorylate the related kinases OSR1 (oxidative stress–responsive kinase 1) and SPAK (STE20/SPS1-related proline/alanine-rich kinase), which control activities and localizations of cation chloride cotransporters such as the sodium chloride cotransporter, and certain ion channels (4–7).

WNK1 is ubiquitously expressed in mammalian tissues. The kinase has been consistently observed to localize to punctate structures scattered throughout the cytoplasm, a population of which is thought to be endocytic vesicles (8–10). Indeed, WNK1 affects the endocytosis of the renal outer medullary K^+ channel by interacting with an endocytic scaffold protein Intersectin (11). WNK1 also promotes the cell surface abundance of the glucose transporters (GLUT) 1 and 4 via the GTPase-activating protein TBC1D4 that regulates the activity of Rab proteins (12, 13). Moreover, we previously found that WNK1 has an inhibitory effect on the activity of class III phosphatidylinositol 3-kinase which is critical in autophagy as part of the protein degradation pathway (14, 15).

The E3 ubiquitin ligase tripartite motif-containing 27 (TRIM27) has emerged as a regulator of endocytic trafficking. TRIM27 localizes to endosomes through interactions with retromer components such as Vps35 and Vps26 (16, 17). The interaction is essential for Wiskott–Aldrich syndrome protein and SCAR homologue (WASH)-mediated actin networks on the surface of endosomes (16, 18). The retromer complex regulates protein recycling from endosomes to the trans-Golgi network or the cell surface (19, 20). Here, we identified an unexpected association between WNK1 and TRIM27, thereby altering WASH ubiquitination. In examining WNK1 actions in triple-negative breast cancer (TNBC) cell lines, we observed differences in epidermal growth factor (EGF) receptor trafficking in cells depleted of WNK1. However, the molecular mechanisms underlying WNK1-mediated endocytic trafficking of growth factor receptors are poorly defined. In this study, we provide evidence for a critical role of WNK1 in regulating endocytic trafficking of a subset of receptor tyrosine kinases (RTKs) in TNBC cells.

Significance

Removal of receptor tyrosine kinase (RTK) from the plasma membrane by endocytosis and subsequent degradation are the major negative regulatory mechanisms to attenuate RTK signaling. RTKs, such as the epidermal growth factor receptor (EGFR) and the TAM (Tyro3-Axl-Mer) receptor kinase AXL, are highly expressed in human cancers. In this study, we describe a function of WNK1 (with-no-lysine 1) in facilitating WASH (Wiskott–Aldrich syndrome protein and SCAR homologue) ubiquitination and activation through regulating TRIM27-USP7 (tripartite motif-containing 27-ubiquitin-specific protease 7) complex formation. The consequences of inhibiting this process are a reduction of endosomal F-actin (filamentous actin) assembly and a disturbance of endocytic sorting of certain RTKs, leading to enhanced degradation of EGFR and AXL in human breast cancer cells.

Author contributions: J.-U.J. designed research; J.-U.J. performed research; J.-U.J. and M.H.C. analyzed data; and J.-U.J. and M.H.C. wrote the paper.

Reviewers: J.S.G., University of California San Diego Medical Center; and A.S., University of Pittsburgh School of Medicine.

The authors declare no competing interest.

[1]To whom correspondence may be addressed. Email: Melanie.Cobb@UTSouthwestern.edu.

This article contains supporting information online at https://www.pnas.org/lookup/suppl/doi:10.1073/pnas.2300310120/-/DCSupplemental.

Published June 12, 2023.

Results

WNK1 Depletion Disrupts WASH Ubiquitination and Endosomal F-Actin (filamentous actin) Nucleation. WNK1 has been linked to alterations in the actin cytoskeleton associated with changes in cell migration, as well as changes in surface localization of a variety of membrane proteins RTKs (21–23). Endosomal sorting and recycling require remodeling of actin networks (24, 25). Actin filaments formed by the assembly of actin monomers are involved in the movement of endocytic vesicles to specific destinations (26, 27). To investigate WNK1 actions in the actin cytoskeleton, we used two different siRNAs (small-interfering RNAs) (siWNK1-1 and siWNK1-2) to knockdown WNK1 expression in two TNBC cell lines, MDA-MB-231 and SUM159. The western blot analysis showed that WNK1 protein was significantly decreased by both siRNAs (*SI Appendix*, Fig. S1*A*). siWNK1-1 (referred to as siWNK1) was used in the following experiments due to its low cytotoxicity and lack of off-target effects as noted in previous studies (14, 22). WNK1 knockdown in the siWNK1-treated cells was further validated by quantitative PCR (qPCR) and by immunofluorescence staining (*SI Appendix*, Fig. S1 *B* and *C*). We first tested whether actin assembly is altered in response to WNK1 depletion. We assessed the ratio of F-actin/G-actin (monomeric globular actin) in siCTRL- or siWNK1-treated TNBC cells. Biochemical analysis of actin fractionation revealed that WNK1-depleted cells displayed a significant decrease in the F/G-actin ratio compared to controls. This result indicates decreased cellular actin polymerization in WNK1 knockdown cells (Fig. 1 *A* and *B*). In the light of previous findings demonstrating that F-actin is highly localized in endosomes and regulates endosomal dynamics for the recycling of cargoes (25, 26), we performed immunofluorescence staining to analyze the intracellular distribution of F-actin on endosomes. In both TNBC cell lines, dense F-actin structures (phalloidin) are highly colocalized with Rab5-positive endosomes (Fig. 1 *C* and *D*; purple staining). The endosomal F-actin clusters in WNK1-depleted cells are almost unnoticeable with faint diffuse staining (Fig. 1 *C* and *D*). The density of endosomal F-actin is significantly reduced by WNK1 knockdown in both TNBC cell lines (Fig. 1 *E* and *F*), leading to the conclusion that WNK1 enables formation of F-actin at endosomes.

Actin filament polymerization and organization are tightly controlled by the actin-related protein 2/3 (Arp2/3), which facilitates F-actin nucleation in cells (28). The activity of Arp2/3 is regulated by WASH (29, 30). WASH has been reported to regulate endosomal actin polymerization via ubiquitination-induced conformational change into an active state (16, 18). We therefore asked whether reduced endosomal F-actin assembly in WNK1-depleted cells is triggered by altered WASH ubiquitination. To investigate this further, we evaluated the degree of WASH ubiquitination with and without stimulation by EGF by coimmunoprecipitation experiments. As shown in Fig. 1 *G* and *H*, WNK1 depletion dramatically reduced endogenous WASH ubiquitination, indicating diminished activity of the WASH complex by WNK1 knockdown. To further validate the possible association of WASH-dependent actin polymerization with endocytosis (16, 24), we performed EGFR (EGF receptor) degradation assays to determine whether depletion of WNK1 affects endosomal trafficking of EGFR. Interestingly, EGFR degradation kinetics upon knockdown of WNK1 were significantly increased in SUM159 cells after 15 min of treatment with EGF as compared with that in siCTRL-treated cells (Fig. 1 *I* and *K*), while EGFR in serum-starved cells was unaltered by WNK1 knockdown (Fig. 1*J*). Similar results were observed in MDA-MB-231 cells, another TNBC cell line (Fig. 1 *L*–*N*). Antibodies, one that targets the extracellular and a second that targets the intracellular domain of the EGFR, reveal similar EGFR degradation kinetics, ruling out the possibility of undetected posttranslationally modified EGFR in WNK1 knockdown cells (Fig. 1 *I* and *L*). WNK1 depletion from A549 human non-small-cell lung cancer cells and HeLa cervical cancer cells also resulted in acceleration of ligand-stimulated EGFR degradation (*SI Appendix*, Fig. S2), indicating that enhanced EGFR degradation by WNK1 depletion is not a cell type–specific result. Taken together, these results highlight the importance of WNK1 in WASH-mediated actin polymerization and protein trafficking.

Loss of WNK1 Increases Susceptibility of TRIM27 to Degradation. It has previously been reported that the E3 ubiquitin ligase TRIM27 regulates WASH ubiquitination, thereby causing its activation (16, 18). Because we observed disruption of WASH ubiquitination by WNK1 knockdown, we analyzed TRIM27 protein in siWNK1-treated MDA-MB-231 and SUM159 cells. Cells were cultured in a medium containing fetal bovine serum (FBS) and transferred to a serum-free medium or stimulated with EGF in the absence of FBS. We did not observe any basal changes in the levels of TRIM27 in WNK1 knockdown cells (Fig. 2 *A*, *B*, *E*, and *F*). Notably, EGF stimulation of WNK1-depleted cells significantly decreased the amount of TRIM27 when compared to siCTRL-treated cells (Fig. 2 *A*, *C*, *E*, and *G*), while the amount of ubiquitin-specific protease 7 (USP7), an upstream regulator of TRIM27 (18, 31), was not changed in siWNK1-treated cells under any of the three culture conditions (Fig. 2 *D* and *H*). Unexpectedly, serum-free conditions also decreased TRIM27 protein (Fig. 2 *A*, *C*, *E*, and *G*), suggesting that TRIM27 turnover is enhanced by dynamic changes of the actin cytoskeleton. Indeed, reorganization of the actin cytoskeleton occurs not only in response to growth factor signaling but also by serum starvation (32, 33). We confirmed that WNK1 depletion in MDA-MB-231 cells did not cause a detectable change of TRIM27 mRNA (Fig. 2*I*), demonstrating that reduced TRIM27 protein caused by WNK1 knockdown is likely to be due to protein destabilization rather than transcriptional effects. Although significant mRNA expression changes were observed in WNK1-depleted SUM159 cells, we have not observed that the changed TRIM27 mRNA leads to changes in TRIM27 protein (Fig. 2 *B* and *I*). Next, we wondered whether WNK1 acts through TRIM27 in regulating WASH activity. We examined the ubiquitination of endogenous WASH in both TNBC cells treated with siCTRL, siWNK1, or siTRIM27 and found that TRIM27-depleted cells displayed strongly attenuated ubiquitination of WASH, similar to that in WNK1-depleted cells (Fig. 2 *J* and *K*). These results suggest that TRIM27 is an important downstream mediator of WNK1-dependent actin polymerization.

We further questioned whether the kinase activity of WNK1 was required for TRIM27 stability. We treated both MDA-MB-231 and SUM159 cells with the pan-WNK kinase inhibitor WNK463 to block WNK1 catalytic activity (34). Surprisingly, this small-molecule compound had no significant effect on either TRIM27 or USP7 turnover compared to Dimethyl sulfoxide (DMSO)-treated cells under all three culture conditions (Fig. 3 *A*–*H*), while WNK463 significantly suppressed phosphorylation of SPAK/OSR1, downstream effectors of WNK1 (Fig. 3 *A* and *E*). We also evaluated the kinetics of EGFR degradation in WNK463-treated TNBC cell lines to determine the possible action of the WNK1-SPAK/OSR1 axis on the EGFR proteolytic process. The kinetics of EGFR degradation in WNK463-treated cells were not significantly different from those in the DMSO control (Fig. 3 *I* and *J*), which indicates that the action of WNK1 in TRIM27 stabilization is independent of its catalytic activity.

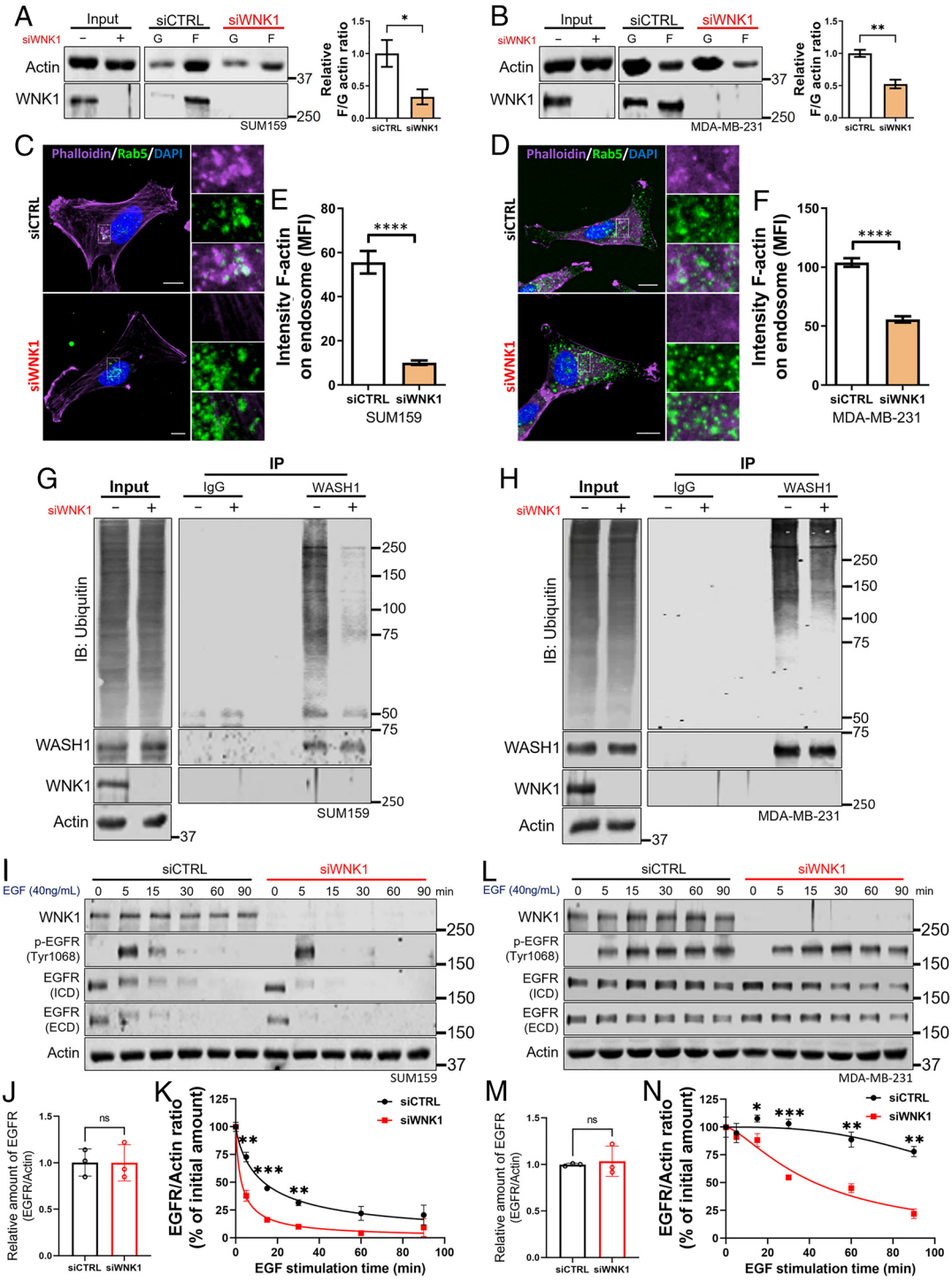

Fig. 1. WNK1 depletion disrupts WASH ubiquitination and endosomal F-actin nucleation. (*A* and *B*) Equal amounts of cell lysates from siCTRL- or siWNK1-treated SUM159 (*A*) or MDA-MB-231 (*B*) cells were fractionated by ultracentrifugation to separate F-actin and G-actin and immunoblotted with the indicated antibodies. The bar graph shows the normalized F/G ratio values. *$P < 0.05$, **$P < 0.01$, unpaired two-tailed *t* test (n = 3). (*C* and *D*) siCTRL- or siWNK1-treated cells were serum starved for 2 h and then stimulated with 40 ng/mL EGF for 10 min (SUM159) or 15 min (MDA-MB-231). Cells were stained using anti-Rab5 (green), phalloidin (purple), and DAPI (blue). Areas within dotted white squares are enlarged and shown on the *Right*. These focal planes were chosen based on Rab5 signals. (Scale bar, 10 μm.) (*E* and *F*) Quantitation of endosomal F-actin intensity on Rab5-positive endosomes in siCTRL- or siWNK1-treated cells. Data are mean ± SEM. of n ≥ 65 cells per condition. ****$P < 0.0001$ (unpaired two-tailed *t* test). MFI, mean fluorescence intensity. (*G* and *H*) SUM159 (*G*) or MDA-MB-231 (*H*) cells were treated with siCTRL or siWNK1 for 72 h and then incubated with MG132 (10 μM) and EGF (40 ng/mL) in the absence of FBS for 6 h. Proteins were immunoprecipitated (IP) with Immunoglobulin G (IgG) or anti-WASH1 and immunoblotted with indicated antibodies. (*I*–*N*) siCTRL- or siWNK1-treated SUM159 (*I*) and MDA-MB-231 (*L*) cells were incubated in serum-deprived medium with cycloheximide (CHX) (50 μg/mL) for 2 h and then stimulated with EGF (40 ng/mL) in the presence of CHX for the indicated times. Lysates were subjected to sodium dodecyl-sulfate polyacrylamide gel electrophoresis (SDS-PAGE) and immunoblotted with indicated antibodies. (*J* and *M*) EGFR quantification after serum starvation for 2 h. ns = no significance. (*K* and *N*) Quantification of EGFR normalized to actin in siCTRL- or siWNK1-treated cells. Data are representative of three independent experiments (mean ± SEM). *$P < 0.05$, **$P < 0.01$, and ***$P < 0.001$, unpaired two-tailed *t* test.

WNK1 Facilitates Formation of the TRIM27-USP7 Complex. To understand the mechanistic link between WNK1 and TRIM27, we first determined whether the two proteins form a complex. Cell lysates of MDA-MB-231 or SUM159 cells were subjected to immunoprecipitation with a WNK1 antibody. TRIM27 was detected in precipitates with endogenous WNK1, suggesting

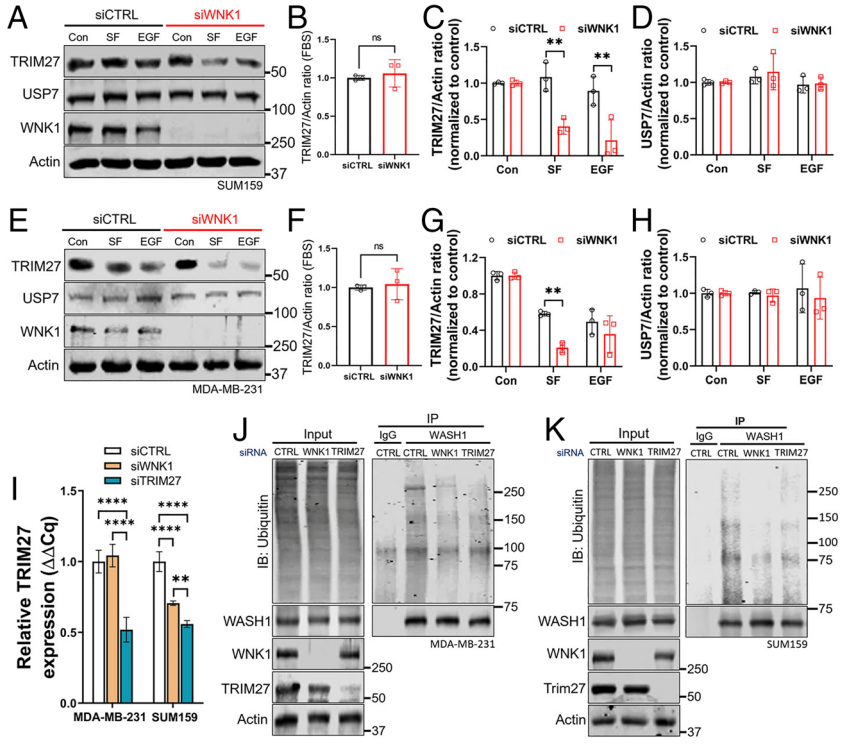

Fig. 2. Loss of WNK1 increases susceptibility of TRIM27 to degradation. (*A–H*) SUM159 (*A*) and MDA-MB-231 (*E*) cells were treated with siCTRL or siWNK1 for 72 h (Con), serum starved for 2 h (SF), and treated with 40 ng/mL of EGF for 15 min (SUM159) or 30 min (MDA-MB-231). (*B* and *F*) Quantification of TRIM27 protein in FBS-containing complete medium (Con) shown in *A* and *E*. Unpaired two-tailed *t* test (mean ± SD), ns = no significance (n = 3). (*C*, *D*, *G*, and *H*) Quantification of TRIM27 (*C* and *D*) or USP7 (*G* and *H*) proteins. Data shown as a ratio of TRIM27 in each condition over the initial amount (Con) in siCTRL- or siWNK1-treated cells (n =3). $^{**}P < 0.01$, unpaired two-tailed *t* test (mean ± SD). (*I*) qPCR of TRIM27 in cells were treated with siCTRL, siWNK1, or siTRIM27. Data are mean ± SD. $^{**}P < 0.01$ and $^{****}P < 0.0001$, one-way analysis ANOVA. (*J* and *K*) MDA-MB-231 (*J*) and SUM159 (*K*) cells were treated with siCTRL, siWNK1, or siTRIM27 for 72 h and then incubated with MG132 (10 μM) and EGF (40 ng/mL) in the absence of FBS for 6 h. Proteins were IP with IgG or anti-WASH1 and immunoblotted with indicated antibodies.

that WNK1 and TRIM27 may form a complex (Fig. 4*A*). In contrast, USP7 and EGFR were barely detectable in the WNK1 immunoprecipitates (Fig. 4*A*). Interaction between WNK1 and TRIM27 was also observed in extracts of the other cell lines, Hela and 293T cells (*SI Appendix*, Fig. S3 *A* and *B*). To further analyze their interaction at a cellular level, we performed a proximity ligation assay (PLA) in both TNBC cell lines to detect in situ protein–protein interactions. Because specific antibodies are not available for immunofluorescence staining of endogenous TRIM27, we used HA-tagged TRIM27-transfected MDA-MB-231 or SUM159 cells and found that WNK1 puncta colocalized with TRIM27 (Fig. 4 *B*, *Left*). Likewise, numerous PLA dots derived by close association between HA-tagged TRIM27 and WNK1 were observed intracellularly (Fig. 4 *B*, *Right*), while the immunoglobulin

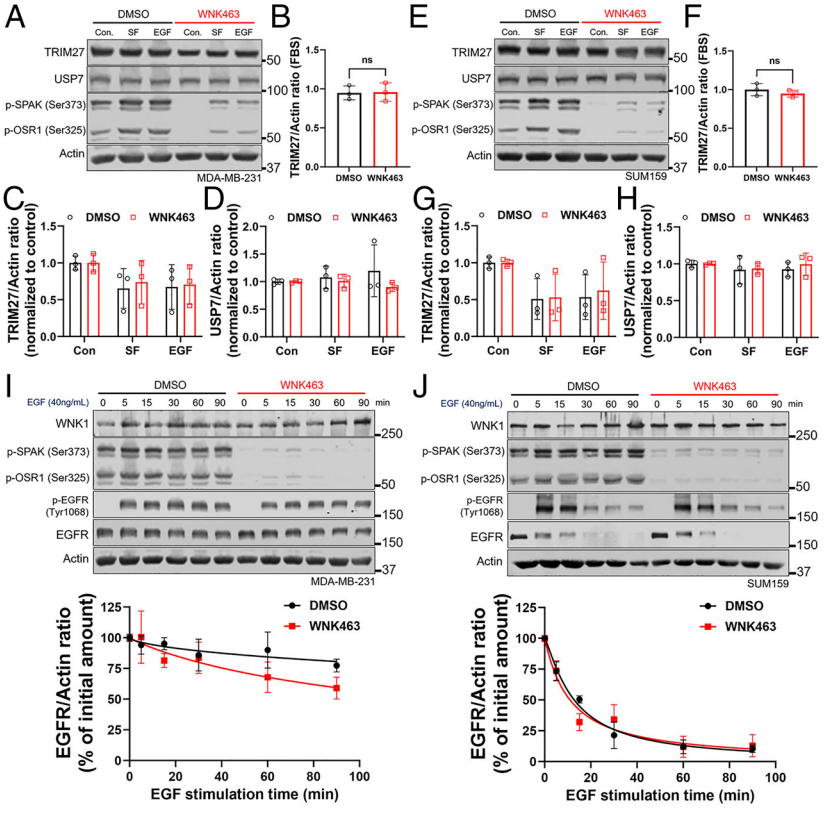

Fig. 3. Inhibition of WNK kinase activity has little effect on TRIM27 or EGFR levels. (*A–H*) MDA-MB-231 (*A*) and SUM159 (*E*) cells pretreated with DMSO or WNK463 (1 μM) for 18 h (Con) were serum starved for 2 h in the presence of DMSO or WNK463 and then stimulated with EGF (40 ng/mL) in the presence of DMSO or WNK463 for 15 min (SUM159) or 30 min (MDA-MB-231). (*B* and *F*) Quantification of TRIM27 protein as in A and E. Statistical significance by an unpaired two-tailed *t* test (mean ± SD), ns = no significance (n = 3). (*C*, *D*, *G*, and *H*) Quantification of TRIM27 (*C* and *D*) or USP7 (*G* and *H*) over the initial amount (Con). Data are mean ± SD of three independent experiments, unpaired two-tailed *t* test. (*I* and *J*) MDA-MB-231 (*I*) and SUM159 (*J*) cells pretreated for 18 h with DMSO or WNK463 (1 μM) were serum starved for 2 h in the presence of CHX (50 μg/mL) and DMSO or WNK463 and then stimulated with EGF (40 ng/mL) in the presence of CHX and WNK463 for 90 min. The *Bottom* panels show EGFR in DMSO- or WNK463 (1 μM)-treated cells following EGF stimulation. Data are representative for three independent experiments (mean ± SEM), unpaired two-tailed *t* test.

G control yielded no signal (Fig. 4 *B*, *Middle*). These results indicate that TRIM27 and endogenous WNK1 colocalize and interact.

TRIM27 forms a complex with USP7 (16, 31). The deubiquitinating enzyme USP7 can remove the ubiquitin from TRIM27 and stabilize it (18, 31). Hence, their interaction is critical for TRIM27 stability and its regulation of ubiquitination-dependent WASH activity (16, 18). As expected, in USP7 knockdown TNBC cells, the amount of TRIM27 protein was remarkably decreased regardless of culture conditions (Fig. 4*C* and *SI Appendix*, Fig. S3*C*), raising the possibility that the downregulation of TRIM27 in WNK1-depleted cells might be due to reduction of its complex formation with the deubiquitinating enzyme. Therefore, we investigated whether WNK1 stabilizes TRIM27 proteins through regulating TRIM27-USP7 complex formation. Immunoprecipitation performed using a USP7 antibody on the lysates of WNK1- or TRIM27-depleted SUM159 cells confirmed that TRIM27 coimmunoprecipitated with USP7 (Fig. 4*D*). Importantly, the amount of coprecipitated TRIM27 was decreased in siWNK1-treated cells, while the amount of precipitated USP7 was not changed (Fig. 4*D*). Reduced complex formation was also observed in MDA-MB-231 and 293T cells by depleting WNK1 (*SI Appendix*, Fig. S3 *D* and *E*), indicating that WNK1 facilitates an interaction between USP7 and TRIM27. Interestingly, however, reduced complex formation in WNK1-depleted cells does not significantly affect total TRIM27 in cells cultured with FBS (Fig. 4 *D*, *Left* and *SI Appendix*, Fig. S3 *D* and *E*). This is apparently due to the absence of stimulus-mediated TRIM27 degradation, as shown by increased degradation of TRIM27 following starvation and EGF stimulation (Fig. 2 *A* and *E*). Furthermore, dissociation of TRIM27 from USP7 caused by WNK1 knockdown was even more pronounced following EGF stimulation (Fig. 4 *D*, *Right*), suggesting WNK1-mediated fine tuning of TRIM27-USP7 complex formation in response to cytoskeletal dynamics. In addition, the PLA confirmed the existence of a TRIM27-USP7 complex in situ, which was reduced in WNK1-depleted cells by least 50% compared to control (Fig. 4*E*). These results demonstrate that WNK1 depletion reduces the formation of the TRIM27-USP7 complex and, thereby, TRIM27 protein.

TRIM27 Knockdown Accelerates RTK Degradation. The preceding results presented WNK1 as a regulator involved in endosomal trafficking of EGFR through regulating TRIM27-mediated ubiquitination of WASH. To directly evaluate the requirement of TRIM27 for EGFR trafficking, we assessed rates of ligand-induced EGFR degradation in TRIM27-depleted cells by western blot analysis. MDA-MB-231 or SUM159 cells were depleted of TRIM27 using siRNA; upon TRIM27 knockdown, the amount of its upstream regulator USP7 did not change significantly (Fig. 5 *A* and *B*). Similar to what occurs in WNK1-depleted cells as shown in Fig. 1 *I*–*N*, TRIM27 knockdown in SUM159 cells accelerated EGFR degradation compared to that in control cells, with only about 20% of the initial EGFR content remaining at 20 min poststimulation (Fig. 5*A*). In MDA-MB-231 cells, more than half of the EGFR was degraded in WNK1 knockdown cells after 1 h of EGF stimulation, whereas 80% was still present in the control cells (Fig. 5*B*). These findings suggest that WNK1 depletion facilitates EGFR degradation through TRIM27 destabilization.

Reduced interaction between TRIM27 and USP7 in WNK1-depleted cells (Fig. 4 *D* and *E* and *SI Appendix*, Fig. S3 *D* and *E*) led us to examine whether USP7 is vital for TRIM27-mediated endosomal trafficking of EGFR. We, therefore, performed EGFR degradation assays in TNBC cells depleted of USP7. As expected, USP7 knockdown dramatically reduced TRIM27 and enhanced EGFR degradation compared to control cells upon EGF stimulation (Fig. 5 *C* and *D*). Considering that TRIM27 depletion accelerated EGFR degradation without a change in USP7 amount (Fig. 5 *A*

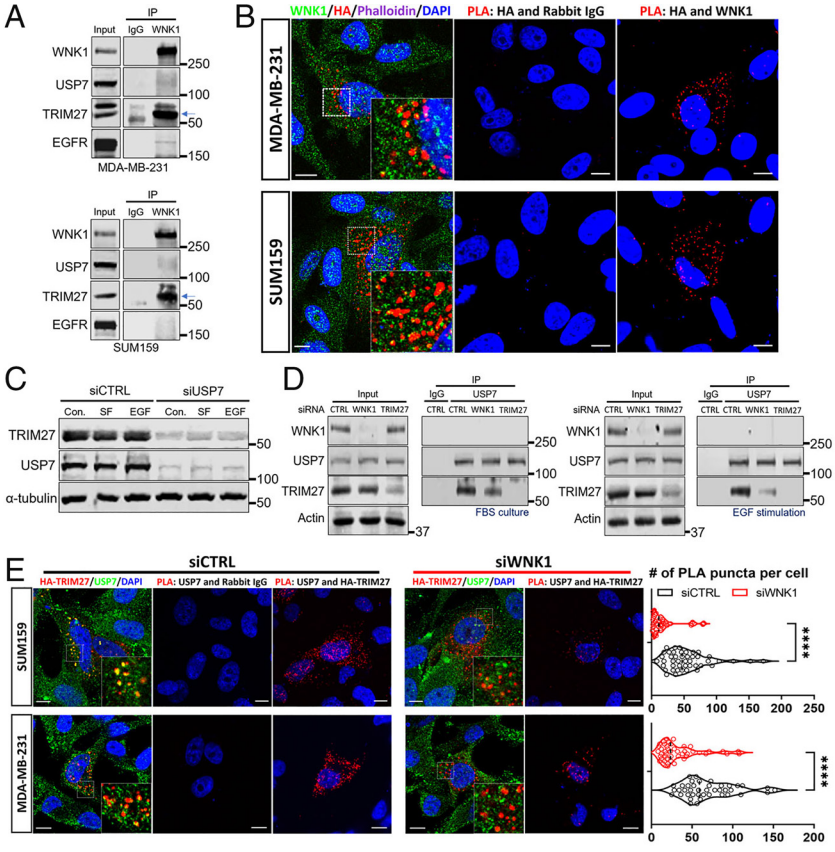

Fig. 4. WNK1 facilitates formation of the TRIM27-USP7 complex. (*A*) MDA-MB-231 (*Upper*) and SUM159 (*Bottom*) lysates were subjected to IP with control IgG or an antibody against endogenous WNK1 and immunoblotted with indicated antibodies. (*B*) MDA-MB-231 and SUM159 cells were transfected with HA-TRIM27. After 48 h, the cells were fixed and stained (*Left*) with anti-WNK1 (green), anti-HA (red), Phalloidin (purple), and DAPI (blue). Images marked with white squares are magnified and shown as *Insets*. Cells were subjected to proximity ligation assay (PLA; red dots) between HA and IgG (*Middle*) or HA and WNK1 (*Right*). (Scale bar, 10 μm.) (*C*) SUM159 cells were treated with siCTRL or siUSP7 for 72 h (Con), serum starved for 2 h (SF), and treated with 40 ng/mL of EGF for 15 min. Lysates were subjected to SDS-PAGE and immunoblotted with indicated antibodies. (*D*) SUM159 cells were treated with siCTRL, siWNK1, or siTRIM27 for 72 h and then incubated in FBS-containing medium (*Left*) or serum-deprived medium with EGF (40 ng/mL) (*Right*) for 4 h. Cell lysates were subjected to IP with IgG or anti-USP7 and immunoblotted with indicated antibodies. (*E*) siCTRL- or siWNK1-treated SUM159 and MDA-MB-231 cells were transfected with HA-TRIM27. After 48 h, cells were fixed and stained with anti-HA (red), anti-USP7 (green), and DAPI (blue). Images marked with white squares are magnified and shown as *Insets*. PLA (red dots) between USP7 and IgG or USP7 and HA was performed in siCTRL- or siWNK1-treated cells. The graph shows the average number of PLA signals per cell (n ≥ 40 cells per condition). ****$P < 0.0001$ (unpaired two-tailed *t* test). (Scale bar, 10 μm.)

and *B*), enhanced EGFR degradation observed in USP7-depleted cells might be attributed to USP7 knockdown-mediated downregulation of TRIM27 (Fig. 5 *C* and *D*).

We next measured effects of WNK1 depletion on mRNAs of selected RTKs known to undergo endosomal trafficking. While most tested mRNAs did not differ significantly between WNK1 knockdown and control MDA-MB-231 cells, mRNAs encoding the EGFR and fibroblast growth factor receptor 1 (FGFR1) were moderately increased in WNK1-depleted cells (Fig. 5*E*), suggesting that WNK1 depletion induced upregulation of EGFR mRNA acts as a compensatory survival mechanism due to accelerated degradation of EGFR protein in TNBC cells. To further assess whether WNK1 plays a selective role in EGFR endosomal trafficking or not, serum-starved siCTRL-, siWNK1-, or siTRIM27-treated TNBC cells were stimulated with FBS, which catalyzes endosomal trafficking of the RTKs. Like EGFR, the AXL RTK (AXL) and FGFR1 have been associated with tumor progression and are continuously internalized and recycled or sorted into late endosomes for degradation (35, 36). Remarkably, enhanced degradation of AXL was also observed in WNK1-depleted TNBC cells (Fig. 5 *F*, *G*, *I*, and *J*). Knockdown of TRIM27 also significantly decreased AXL by 30% in SUM159 cells and 60% in MDA-MB-231 cells as compared to controls at 30 min poststimulation but to a lesser extent than WNK1 knockdown (Fig. 5 *F*, *G*, *I*, and *J*). This difference suggests that other complex actions of WNK1 may be involved in processing these RTKs (14, 37). These results are consistent with our previous study showing that WNK1 depletion suppresses expression of AXL protein without reducing its mRNA (22). By contrast, FGFR protein levels were unchanged by knockdown of either WNK1 or TRIM27 in both TNBC cells (Fig. 5 *F*, *H*, *I*, and *K*), although its mRNA level was slightly increased (Fig. 5*E*). Collectively, these data suggest that WNK1 regulation of TRIM27 turnover plays selective roles for specific surface receptors in specific cell types rather than globally controlling the fate of surface receptors in cells stimulated with growth factors or serum.

Loss of WNK1 Directs Proteolytic Processing of EGFR. In mammalian cells, lysosomal and proteasomal degradation pathways are two major proteolytic systems controlling protein turnover. Both pathways participate in ligand-stimulated EGFR degradation (38, 39). Next, we tested which of these proteolytic pathways for EGFR degradation was affected by WNK1 depletion. MDA-MB-231 and SUM159 cells were treated with EGF in the presence or absence of the lysosome inhibitor bafilomycin A1 or the proteasome inhibitor MG132. We found that either proteasome or lysosome inhibitors efficiently suppressed EGFR degradation upon EGF stimulation; in particular inhibition by bafilomycin A1 led to a greater accumulation of EGFR (Fig. 6 *A*–*D*), indicating that ligand-stimulated EGFR is degraded significantly by the lysosome-dependent pathway. Interestingly, neither lysosomal nor proteasomal inhibitors fully prevented the decrease in EGFR in WNK1-depleted cells (Fig. 6 *A*–*D*). These results suggest that WNK1 is a crucial factor regulating EGFR stability upon EGF stimulation.

Activated RTKs such as ligand-bound EGFR are endocytosed and sequestered within early endosomes and then actively sorted into either recycling or late endosomes for recycling or lysosomal degradation, respectively (40, 41). These processes influence the total number of free receptors on the cell surface. Altered kinetics of EGFR degradation might be caused by changes in internalization or endosomal trafficking. Therefore, we next performed cell surface biotinylation assays (42) to determine whether WNK1 depletion influenced endosomal trafficking of EGFR. We detected similar amounts of biotinylated surface EGFR after serum starvation in siCTRL- and siWNK1-treated cells (Fig. 6 *E*, *F*, *H*, and *I*). Time course analysis in the assays to measure the remaining surface levels of EGFR showed that EGF stimulation in WNK1-depleted cells induced a continuous reduction of EGFR at the cell surface, similar to that observed in the control cells (Fig. 6 *E* and *G*), indicating that loss of WNK1 has no apparent effect on the internalization event during ligand-induced endocytosis of EGFR. As the acceleration of EGFR degradation in WNK1 knockdown cells is little influenced by its internalization, changes in postinternalization events are implicated. We examined the amount of EGFR that was internalized upon EGF stimulation. Both siCTRL- and siWNK1-treated cells exhibited similar accumulation kinetics of EGFR within the first 15 min (Fig. 6 *H* and *J*). However, later kinetics of accumulation were dramatically reduced in WNK1-depleted cells, while a noticeable accumulation of the internalized EGFR was observed in control cells (Fig. 6 *H* and *J*), supporting the idea that WNK1 is responsible for controlling EGFR stability. Together, these results suggest that WNK1 influences endosomal trafficking of EGFR after its internalization.

Loss of WNK1 Decreases Colocalization of Rh-EGF (Rhodamine-conjugated EGF) with Rab11. The actin network is important for appropriate trafficking of endosomal vesicles to their specific destinations (26, 27). As shown in Figs. 1 and 6, enhanced EGFR degradation in WNK1 knockdown cells is at least in part due to the impairment of actin polymerization, which obstructs trafficking. Hence, we performed EGF pulse–chase experiments using a fluorescently labeled EGF to monitor the alteration of EGFR trafficking caused by WNK1 depletion at the single-cell level. In control cells, we found that the Rh-EGF-positive puncta are internalized, accumulated in the cytoplasm after 15 min, and gradually concentrated in a large cluster of vesicles within the perinuclear region (Fig. 7*A*), where activated EGFR is thought to encounter phosphatases to be inactivated (43). In contrast, Rh-EGF signals in WNK1-depleted cells at 60 min after the pulse are still detected throughout the cytoplasm, and the puncta are substantially smaller, consequently resulting in more puncta than are in cells expressing siCTRL (Fig. 7 *A* and *B*). As compared to control cells, Rh-EGF puncta in WNK1 knockdown cells are more scattered throughout the cytoplasm with the appearance of discrete vesicles instead of accumulating around the nucleus (Fig. 7*C*). Furthermore, some Rh-EGF puncta within the perinuclear region are near WNK1 puncta (Fig. 7 *C*, *Left*); however, EGF stimulation did not trigger detectable changes in WNK1 localization (*SI Appendix*, Fig. S4). Consistent with trafficking patterns of Rh-EGF, immunofluorescent staining of EGFR confirmed its perinuclear accumulation after 30 min of EGF treatment in MDA-MB-231 cells (Fig. 7*D* and *SI Appendix*, Fig. S5*A*). The perinuclear accumulation of EGF-stimulated EGFR is significantly diminished by WNK1 depletion (Fig. 7*D* and *SI Appendix*, Fig. S6*A*). Similar observations were made when transferrin trafficking was measured in MDA-MB-231 cells depleted of WNK1 (*SI Appendix*, Fig. S6). In SUM159 cells, EGFR accumulated at the perinuclear region disappeared by 90 min after EGF stimulation, indicating that SUM159 cells have a relatively rapid process of EGFR sorting for its degradation, which was accelerated by WNK1 knockdown (*SI Appendix*, Fig. S5 *B* and *C*). These observations suggest that WNK1 is critical for proper endosomal trafficking of EGFR to the perinuclear region.

After ligand binding, endocytic vesicles converge toward early endosomes by fusion (44) and are transported toward the perinuclear region (43). Recycling endosomes are mostly clustered in the perinuclear endocytic recycling compartment (45). To further investigate the disruption of perinuclear accumulation of EGFR in WNK1-depleted cells, we explored cellular localization of Rh-EGF in TNBC cells. Serum-starved MDA-MB-231

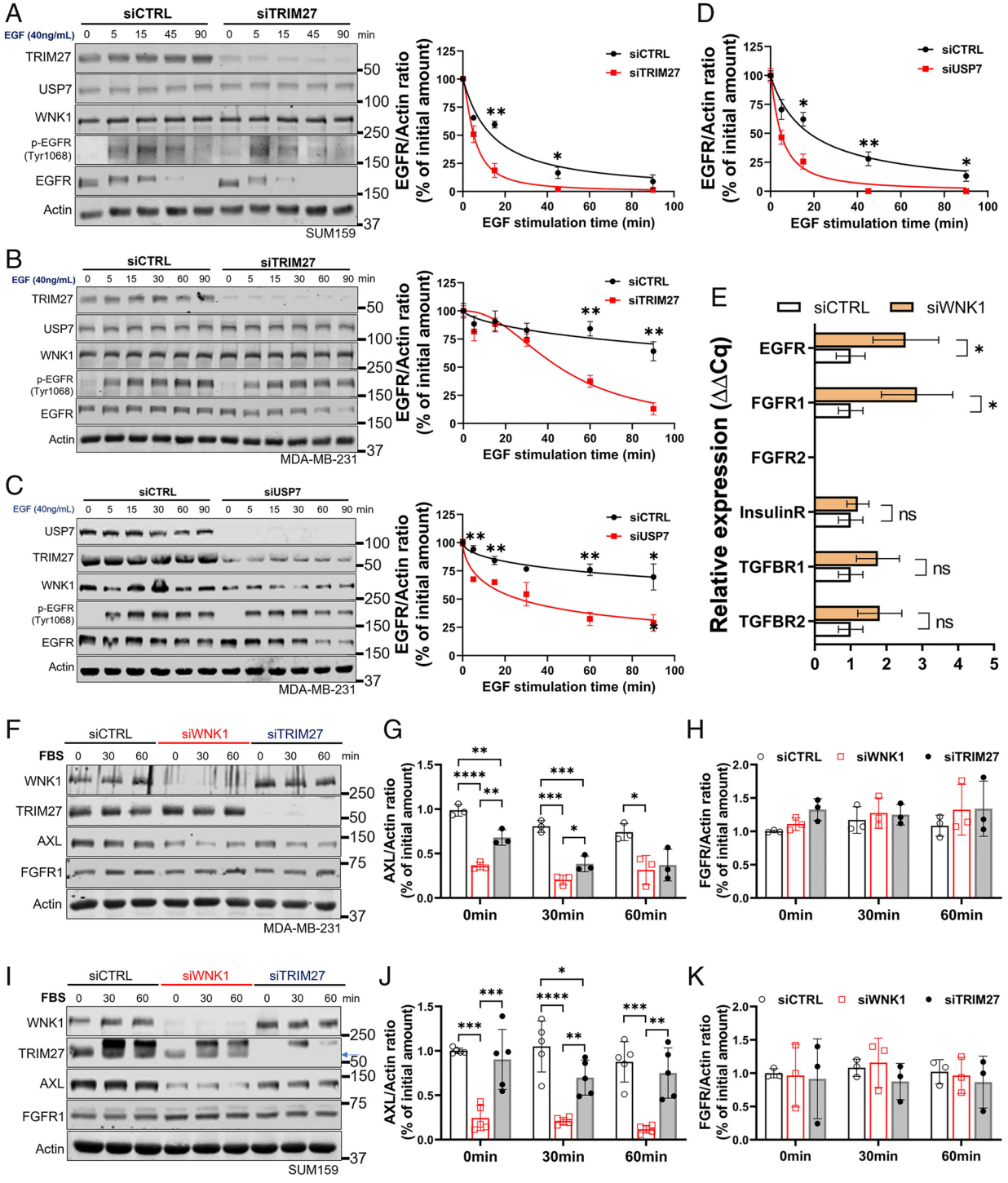

Fig. 5. TRIM27 knockdown accelerates RTK degradation. (*A* and *B*) SUM159 (*A*) and MDA-MB-231 (*B*) cells were treated with siCTRL or siTRIM27. After 72 h incubation, the cells were incubated in serum-deprived medium with CHX (50 μg/mL) for 2 h and then stimulated with EGF (40 ng/mL) in the presence of CHX. *Right* panels, Quantification of three independent experiments. EGFR at each time was normalized against that at 0 min (mean ± SEM), $*P < 0.05$ and $**P < 0.01$, unpaired two-tailed *t* test. (*C* and *D*) siCTRL- or siUSP7-treated MDA-MB-231 (*C*) and SUM159 (*D*) cells were serum starved with CHX (50 μg/mL) for 2 h and stimulated with EGF (40 ng/mL) in the presence of CHX for indicated times. Graphs show the relative amount of EGFR. Data are representative of three separate experiments and are mean ± SEM. $*P < 0.05$ and $**P < 0.01$, unpaired two-tailed *t* test. (*E*) qPCR of RTK expression in siCTRL- or siWNK1-treated MDA-MB-231 cells. Data are mean ± SD. $**P < 0.01$, unpaired two-tailed *t* test. (*F–K*) siCTRL-, siWNK1-, or siTRIM27-treated MDA-MB-231 (*F–H*) and SUM159 (*I–K*) cells were cultured in serum-deprived medium for 2 h and then stimulated with 10% FBS. The amount of AXL (*G* and *J*) or FGFR1 (*H* and *K*) present in each time point normalized to that at 0 min (mean ± SD), $*P < 0.05$, $**P < 0.01$, $***P < 0.001$, and $****P < 0.0001$, one-way analysis ANOVA.

and SUM159 cells were treated with Rh-EGF and stained with endosomal markers, including the early endosome marker Rab5, the late endosome marker Rab7, and the recycling endosome marker Rab11. Consistent with the initial results from Fig. 7*A*, most of the Rh-EGF signals after a 15-min chase were detected in the form of large punctate structures within the perinuclear region in MDA-MB-231 cells (Fig. 7*E*). Interestingly, internalized Rh-EGF puncta in the perinuclear area are largely

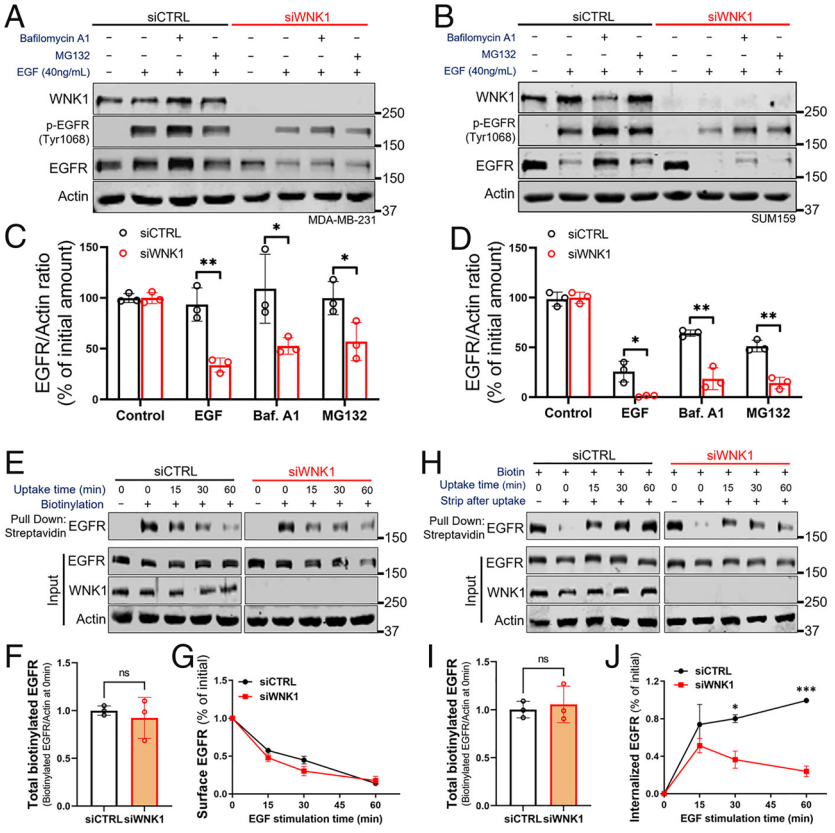

Fig. 6. Loss of WNK1 directs proteolytic processing of EGFR. (*A*–*D*) siCTRL- or siWNK1-treated MDA-MB-231 (*A* and *C*) and SUM159 (*B* and *D*) were starved and exposed to MG132 (10 μM) or bafilomycin A1 (50 nM) in the presence of CHX (50 μg/mL) for 2 h and then stimulated with EGF (40 ng/mL) in the presence of CHX and MG132 or bafilomycin A1 for 30 min (SUM159) or 60 min (MDA-MB-231). Quantification of EGFR protein is shown in *C* (MDA-MB-231) and *D* (SUM159). Results are expressed as mean ± SD. $*P < 0.05$ and $**P < 0.01$, unpaired two-tailed *t* test. (*E*) siCTRL- or siWNK1-treated MDA-MB-231 cells were incubated in serum-deprived medium with CHX (50 μg/mL) for 2 h and then stimulated with EGF (40 ng/mL in the presence of CHX. Cells were surface biotinylated at 4 °C, and labeled proteins were pulled down with NeutrAvidin beads, analyzed by SDS-PAGE followed by immunoblotting. (*F*) Quantification of total biotinylated EGFR normalized to actin before EGF stimulation (0 min). Unpaired two-tailed *t* test (mean ± SD), ns = no significance (n = 3). (*G*) Quantification of surface biotinylated EGFR over time was normalized against the data at 0 min (mean ± SEM), unpaired two-tailed *t* test. (*H*) Serum-starved siCTRL- or siWNK1-treated MDA-MB-231 were surface biotinylated at 4 °C and incubated with EGF (40 ng/mL), CHX (50 μg/mL), and chloroquine (50 μM) at 37 °C for the indicated periods of time to allow endocytosis of the biotinylated surface EGFR. After stripping the remaining biotin from the cell surface, internalized biotinylated EGFR was pulled down with NeutrAvidin beads and subjected to SDS-PAGE and immunoblotted with the indicated antibodies. (*I*) Quantification of total biotinylated EGFR normalized to actin before stripping (0 min without stripping). Unpaired two-tailed *t* test (mean ± SD), ns = no significance (n = 3). (*J*) Quantification of internalized biotinylated EGFR over time was normalized to data at 0 min without stripping (mean ± SEM), $*P < 0.05$ and $***P < 0.001$, unpaired two-tailed *t* test.

overlapped with Rab11, as compared to Rab5- and Rab7-positive endosome (Fig. 7 *E* and *F*), indicating that ligand-stimulated EGFR in MDA-MB-231 cells is mainly trafficked toward the endosomal recycling pathway rather than the late endosome for degradation. Notably, WNK1 depletion caused a significant decrease in colocalization of Rh-EGF with Rab11; a significant increase in the colocalization between Rh-EGF and Rab7 was observed in WNK1-depleted cells compared to control cells (Fig. 7 *E* and *F*). A similar trend was also observed in WNK1-depleted SUM159 cells after 10 min of Rh-EGF chase (*SI Appendix*, Fig. S7). The two cell lines show distinctly different endosomal distributions of Rh-EGF which may be attributed to the difference in degradation kinetics between them (Fig. 1 *K* and *N*). Additionally, WNK1 knockdown changes the subcellular distribution of Vps35 from predominantly perinuclear staining to dispersed puncta throughout the cytoplasm, clearly indicating disrupted retrograde trafficking in WNK1-depleted cells (*SI Appendix*, Fig. S8). Taken together, these results indicate that WNK1 adjusts EGFR fate by promoting recycling rather than degradation in TNBC cells.

Discussion

The complex of TRIM27 with its ubiquitin peptidase USP7 was shown to control endosomal actin polymerization through ubiquitination of the WASH complex, facilitating endosomal trafficking (16, 18). The endosomal localization of TRIM27 is facilitated by interactions with retromer elements such as Vps35 and Vps26 (16–18). Although the deubiquitylation of TRIM27 by binding USP7 for WASH-mediated precise actin polymerization has previously been identified, how their complex formation is regulated remains obscure. In this study, we identified an unrecognized function of WNK1 in stabilizing TRIM27 through facilitating the formation of the TRIM27-USP7 complex to function in actin assembly for endocytosis (Fig. 7*G*).

Assembled actin filaments at the surface of endosomes participate in multiple steps of endocytic trafficking such as membrane fission and internalization of endocytic vesicles from the plasma membrane (46). Here, we examined actin assembly on early endosomes following EGF stimulation and found that WNK1 knockdown decreases the F-actin density around early endosomes accompanied by enhanced ubiquitination of the actin nucleation promoting factor WASH (Fig. 1). In this context, the E3 RING (Really Interesting New Gene) ubiquitin ligase TRIM27 is emerging as a key player to mediate polyubiquitylation of WASH (16). The RING adaptor MAGE-L2, along with USP7 and TRIM27, are recruited to retromer-positive endosomes, where they form a complex that alters the conformation of WASH1. This complex catalyzes the formation of K63-linked polyubiquitin chains at Lys-220 (16, 18), which are essential for multiple cellular functions (47). Because of the spatiotemporal dynamics of the actin filaments, it is possible that transient enrichment of K63-linked polyubiquitylation of WASH occurs during ligand stimulation. Furthermore, WASH is not solely ubiquitinated via the K63-linkage; thus, other types of ubiquitination, such as K48, may collaborate in regulation. This is a problem which warrants further investigation.

The uptake of surface EGFR after ligand stimulation in WNK1-depleted cells closely resembled that of wild-type cells (Fig. 6 *E* and *G*), suggesting that the levels of F-actin on endosomes are not likely to engage with initial internalization. The internalized endosomes are dispersed throughout the cytoplasm (Fig. 7 and *SI Appendix*, Fig. S5), which likely corresponds with defective trafficking of early endosomes due to reduced WASH-mediated actin assembly on these endosomes. This is consistent with the observation that decreased endosomal F-actin nucleation by loss of TRIM27 or USP7 leads to the dispersion of EEA1-positive puncta

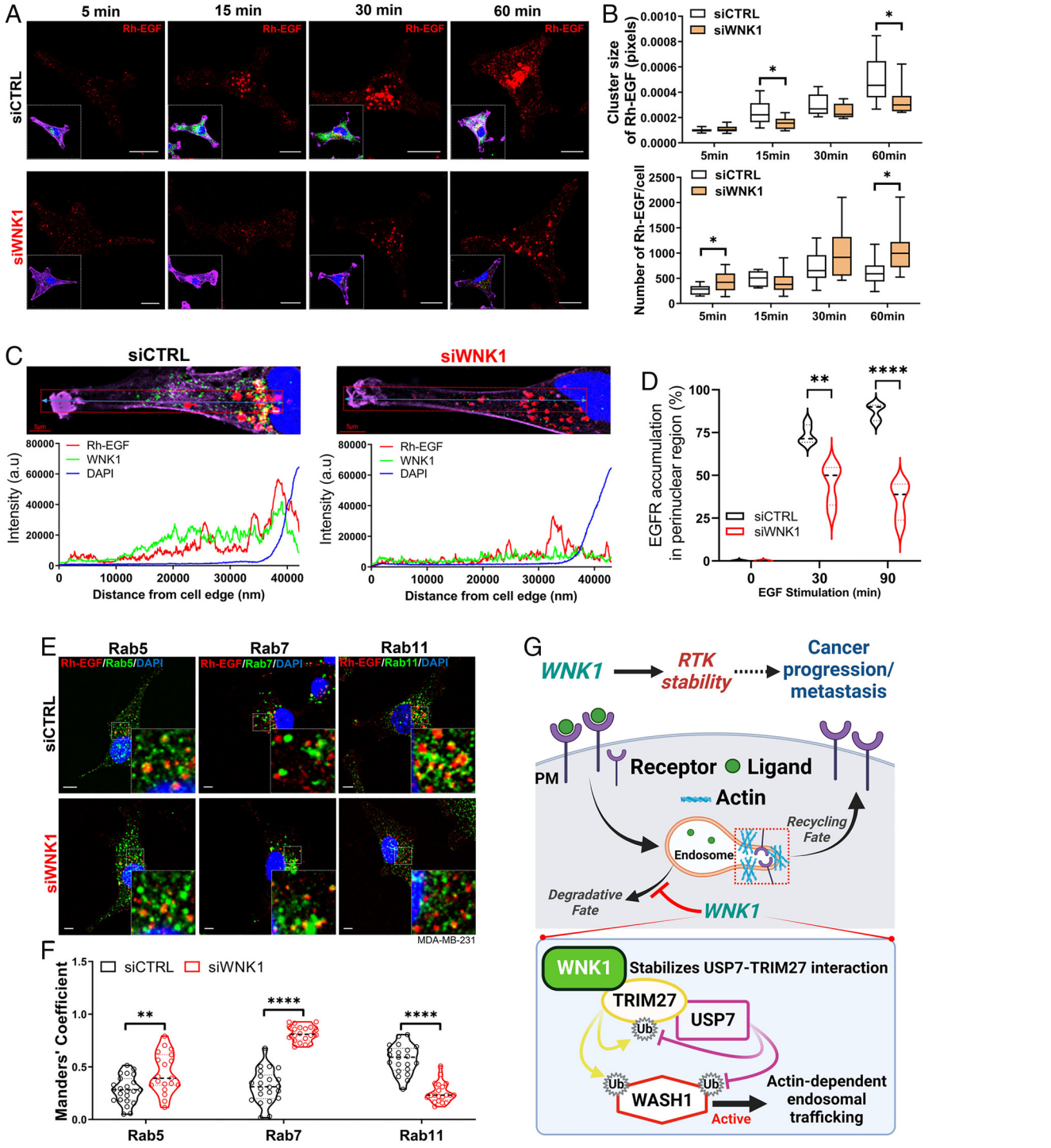

Fig. 7. Loss of WNK1 decreases colocalization of Rh-EGF with Rab11. (*A*) MDA-MB-231 cells treated with siCTRL or siWNK1 were serum starved for 2 h and then pulsed with Rh-EGF (10 ng/mL) for 5 min and chased over time at 37 °C. *Insets* are merged images of each. Rh-EGF (red), anti-WNK1 (green), DAPI (blue), and phalloidin (purple). (Scale bar, 10 μm.) (*B*) Sizes (*Upper*) and numbers (*Lower*) of the Rh-EGF-positive clusters in individual cells were quantified using the Analyze Particles function in ImageJ. Data are shown as boxes and whiskers with all the individual data points (n = 10 cells per condition). **P* < 0.05, unpaired two-tailed *t* test. (*C*) Fluorescence intensity profile plot of Rh-EGF in siCTRL- or siWNK1-treated MDA-MB-231 cells. Graphs show fluorescence intensity, expressed in arbitrary units (a.u.), of Rh-EGF (red), anti-WNK1 (green), and DAPI (blue) along the line arrows in the *Upper* images. (Scale bar, 5 μm.) (*D*) Serum-starved MDA-MB-231 cells treated with siCTRL or siWNK1 were stimulated with EGF (40 ng/mL) over time and then fixed and stained with anti-EGFR (green), anti-WNK1 (red), DAPI (blue), and phalloidin (purple) (*SI Appendix*, Fig. S6). Quantification shows percentage of cells with EGFR puncta (>2.0 μm diameter) in perinuclear region. Data are shown as violin plots (n ≥ 63 cells per condition). ***P* < 0.01 and *****P* < 0.0001, unpaired two-tailed *t* test. (*E*) Serum-starved siCTRL- or siWNK1-treated MDA-MB-231 cells were pulsed with Rh-EGF (red; 10 ng/mL) for 5 min and chased for 15 min. The cells were fixed and stained with antibodies against endosome markers (Rab5, Rab7, or Rab11; green) and DAPI (blue). Images marked with white squares are magnified and shown as *Insets*. (Scale bar, 5 μm.) (*F*) Bar graph showing Manders' coefficients for colocalization of endosome marker and Rh-EGF. Data are shown as violin plots with all the individual data points (n ≥ 19 cells per condition). ***P* < 0.01 and *****P* < 0.0001, unpaired two-tailed *t* test. (*G*) A schematic illustration of WNK1 regulating WASH-mediated actin dynamics via TRIM27 stabilization, resulting in proper endosomal trafficking of RTK.

(16, 18). Precise actin assembly seems to act in the appropriate positioning and transport of endosomes to prevent entry of the vesicles into the degradative pathway (16, 48). Supporting this model, EGFR degradation was significantly increased in cells depleted of WNK1, as well as in TRIM27- or USP7-depleted cells (Figs. 1 *I*–*N* and 5 *A*–*D*). Interestingly, the enhanced degradation in WNK1 knockdown cells was not fully restored by either lysosome or proteasome inhibitors, but was rescued in control cells treated with them, suggesting that depletion of WNK1 may result in a failure of endocytic vesicles to traffic to the proper cellular compartment. In the context of a degradation abnormality, it is possible that an aberrant position of endosomal vesicles caused by depletion of the WNK1-TRIM27 axis triggers unusual proteolytic processes such as caspases or serine proteases that do not predominate in other states (49, 50).

Although WNK1 has been implicated in regulating the endocytosis of ion channels and GLUT on the cell surface (11–13), its functions in the sorting and delivery of surface RTKs for recycling or degradation are unexplored. Here, we provide evidence that WNK1-dependent actin dynamics influence postinternalization events. Unexpectedly, the catalytic activity of WNK1 is not required for TRIM27 stability and regulation of endosomal trafficking of EGFR (Fig. 3). Thus, WNK1 acts as a scaffold protein that positively contributes to the integrity of the TRIM27-USP7 complex, resulting in increased stability of TRIM27 and WASH-dependent actin polymerization. Similarly, other protein kinases have been described as assembly factors, via catalytic activity–independent functions (51, 52). In the case of WNK1, multiple activity–independent, scaffolding functions have been reported (53). Endosomal trafficking dependent on WNK1-TRIM27 appears to be limited to certain RTKs, including EGFR and AXL (Fig. 5 *F* and *I*). Further, it has been reported that EGFR forms functional heterodimers with AXL (35, 54), suggesting that endocytic events involving these RTKs could share some common regulated steps, e.g., via WNK1 and TRIM27. It will be critical in future studies to determine which other RTKs or surface receptors are regulated by this mechanism.

Growth factors, serum starvation, or mechanical stimulation induce changes in the actin cytoskeleton structure that influences the endocytic process (32, 33, 55). We found that serum starvation, with or without EGF, decreased TRIM27 protein in WNK1-depleted cells (Fig. 2 *A*–*H*). Reduced TRIM27 was clearly linked with loss of a complex with USP7, which protects TRIM27 from autoubiquitination via its RING finger domain and proteasomal degradation (18, 31). However, TRIM27 protein remains unchanged in WNK1-depleted cells maintained in FBS (Fig. 2 *B* and *F*), even though it does not form a stable complex with USP7 under this condition (Fig. 4 *D*, *Left*). This suggests that cellular perturbations by growth factors or serum deprivation promote TRIM27 autoubiquitination and degradation. Therefore, these cellular stimuli in WNK1 knockdown cells likely allow TRIM27 to be readily degraded in the absence of its deubiquitinating enzyme, leading to a reduction of total TRIM27 (Fig. 4 *D*, *Right*). More recently, it has been shown that starvation facilitates interaction between TRIM27 and the serine/threonine kinase ULK1, which is a key enzyme in autophagy initiation (56), while a normal culture medium containing FBS diminishes the interaction (57). We have previously shown that ULK1 expression can be regulated by WNK1 (14). Thus, it is possible that WNK1 regulates the availability of TRIM27 and its interacting partners such as ULK1 to stabilize TRIM27 protein.

Aberrant RTK signaling is frequently observed in cancers and dysregulated RTK trafficking promotes tumorigenic and metastatic capacities of cancer cells by activating downstream signaling cascades linked to poor outcomes (58), suggesting that interfering with RTK expression and localization may have therapeutic value in cancer cells. Importantly, recent studies revealed that TRIM27 is elevated in human cancers (59) and is required for TNBC tumor growth in mouse xenograft models (60). WNK1 also has been linked to multiple cancers (61). Our previous work demonstrated that WNK1 regulates endothelial cell migration and angiogenesis by regulating downstream signaling proteins (62). WNK inhibition reduced the invasive ability and the size of orthotopic tumors from TNBC cells compared to those in control animals (22), suggesting that WNK1 is involved in TNBC tumor progression and invasion. In fact, as compared to the control, we found that depleting WNK1 expression significantly decreased the number of invasive cells in the 3D collagen matrix invasion assay (*SI Appendix*, Fig. S9). Surprisingly, TRIM27 depletion largely prevented invasion (*SI Appendix*, Fig. S9). Thus, the impact of WNK1-TRIM27 on endosomal trafficking may influence RTK-driven oncogenic processes (Fig. 7*G*). Future studies are needed to clarify the physiological significance of the WNK1-TRIM27 axis in TNBC cells.

In conclusion, our results uncovered the importance of WNK1 in regulating RTK turnover. We show here that WNK1 acts as a scaffold protein for stabilization of the E3 ubiquitin ligase TRIM27, resulting in WASH-dependent actin assembly essential for appropriate endosomal trafficking dynamics.

Materials and Methods

The detailed methods for Antibodies and Reagents, Cell Culture and Treatment, siRNA, Western Blot Analysis and Immunoprecipitation, Cell Surface Biotinylation Assay, EGFR Degradation Assay, F-actin and G-actin Fractionation, Immunofluorescence Staining, PLA, EGF Pulse–chase Assay, qPCR, Transferrin Trafficking Assay, Three-dimensional Collagen Invasion Assay, and Statistical Analyses are described in *SI Appendix*.

Data, Materials, and Software Availability. All study data are included in the article and/or *SI Appendix*.

ACKNOWLEDGMENTS. We thank former and current members of the Cobb lab for their advice and assistance with specific aspects of this project and Dr. Joseph Albanesi (Department of Pharmacology, UT Southwestern) for discussions. We are grateful to Dr. Szu-Wei Tu, who suggested the initial idea for this project. We would also like to thank Dr. Angelique Whitehurst (Department of Pharmacology, UT Southwestern) for providing the HA-TRIM27 construct and Dionne Ware for administrative assistance. This work was supported by a grant from the NIH (HL147661) and the Welch Foundation (I-1243) to M.H.C. and the Simmons Comprehensive Cancer Center NCI grant (P30 CA142543) for support of the UTSW Live Cell Imaging Core. J.-U.J. was supported by a training grant from the Cancer Prevention and Research Institute of Texas, RP 210041.

Author affiliations: [a]Department of Pharmacology, University of Texas Southwestern Medical Center, Dallas, TX 75390

1. B. Xu *et al.*, WNK1, a novel mammalian serine/threonine protein kinase lacking the catalytic lysine in subdomain II. *J. Biol. Chem.* **275**, 16795–16801 (2000).
2. A. Zagorska *et al.*, Regulation of activity and localization of the WNK1 protein kinase by hyperosmotic stress. *J. Cell Biol.* **176**, 89–100 (2007).
3. B. E. Xu *et al.*, WNK1 activates SGK1 to regulate the epithelial sodium channel. *Proc. Natl. Acad. Sci. U.S.A.* **102**, 10315–10320 (2005).
4. A. N. Anselmo *et al.*, WNK1 and OSR1 regulate the Na+, K+, 2Cl- cotransporter in HeLa cells. *Proc. Natl. Acad. Sci. U.S.A.* **103**, 10883–10888 (2006).

5. C. Richardson *et al.*, Activation of the thiazide-sensitive Na+-Cl- cotransporter by the WNK-regulated kinases SPAK and OSR1. *J. Cell Sci.* **121**, 675–684 (2008).
6. K. Piechotta, J. Lu, E. Delpire, Cation chloride cotransporters interact with the stress-related kinases Ste20-related proline-alanine-rich kinase (SPAK) and oxidative stress response 1 (OSR1). *J. Biol. Chem.* **277**, 50812–50819 (2002).
7. B. F. Dowd, B. Forbush, PASK (proline-alanine-rich STE20-related kinase), a regulatory kinase of the Na-K-Cl cotransporter (NKCC1). *J. Biol. Chem.* **278**, 27347–27353 (2003).
8. S. W. Tu, A. Bugde, K. Luby-Phelps, M. H. Cobb, WNK1 is required for mitosis and abscission. *Proc. Natl. Acad. Sci. U.S.A.* **108**, 1385–1390 (2011).
9. C. R. Boyd-Shiwarski *et al.*, WNK kinases sense molecular crowding and rescue cell volume via phase separation. *Cell* **185**, 4488–4506.e20 (2022), 10.1016/j.cell.2022.09.042.
10. B. H. Lee *et al.*, WNK1 phosphorylates synaptotagmin 2 and modulates its membrane binding. *Mol. Cell* **15**, 741–751 (2004).
11. G. He, H. R. Wang, S. K. Huang, C. L. Huang, Intersectin links WNK kinases to endocytosis of ROMK1. *J. Clin. Invest.* **117**, 1078–1087 (2007).
12. A. I. Mendes, P. Matos, S. Moniz, P. Jordan, Protein kinase WNK1 promotes cell surface expression of glucose transporter GLUT1 by regulating a Tre-2/USP6-BUB2-Cdc16 domain family member 4 (TBC1D4)-Rab8A complex. *J. Biol. Chem.* **285**, 39117–39126 (2010).
13. J. H. Kim *et al.*, WNK1 kinase is essential for insulin-stimulated GLUT4 trafficking in skeletal muscle. *FEBS Open Bio.* **8**, 1866–1874 (2018).
14. S. Gallolu Kankanamalage *et al.*, Multistep regulation of autophagy by WNK1. *Proc. Natl. Acad. Sci. U.S.A.* **113**, 14342–14347 (2016).
15. S. Gallolu Kankanamalage *et al.*, WNK1 is an unexpected autophagy inhibitor. *Autophagy* **13**, 969–970 (2017).
16. Y. H. Hao *et al.*, Regulation of WASH-dependent actin polymerization and protein trafficking by ubiquitination. *Cell* **152**, 1051–1064 (2013).
17. H. X. Zhang *et al.*, TRIM27 mediates STAT3 activation at retromer-positive structures to promote colitis and colitis-associated carcinogenesis. *Nat. Commun.* **9**, 3441 (2018).
18. Y. H. Hao *et al.*, USP7 acts as a molecular rheostat to promote WASH-dependent endosomal protein recycling and is mutated in a human neurodevelopmental disorder. *Mol. Cell* **59**, 956–969 (2015).
19. M. N. Seaman, J. M. McCaffery, S. D. Emr, A membrane coat complex essential for endosome-to-Golgi retrograde transport in yeast. *J. Cell Biol.* **142**, 665–681 (1998).
20. C. Burd, P. J. Cullen, Retromer: A master conductor of endosome sorting. *Cold Spring Harb. Perspect. Biol.* **6**, a016774 (2014).
21. Z. Liu *et al.*, Control of podocyte and glomerular capillary wall structure and elasticity by WNK1 kinase. *Front. Cell Dev. Biol.* **8**, 618898 (2020).
22. A. B. Jaykumar *et al.*, WNK1 enhances migration and invasion in breast cancer models. *Mol. Cancer Ther.* **20**, 1800–1808 (2021), 10.1158/1535-7163.MCT-21-0174.
23. N. Mausbacher, T. B. Schreiber, H. Daub, Glycoprotein capture and quantitative phosphoproteomics indicate coordinated regulation of cell migration upon lysophosphatidic acid stimulation. *Mol. Cell Proteomics* **9**, 2337–2353 (2010).
24. E. MacDonald *et al.*, HRS-WASH axis governs actin-mediated endosomal recycling and cell invasion. *J. Cell Biol.* **217**, 2549–2564 (2018).
25. M. A. Puthenveedu *et al.*, Sequence-dependent sorting of recycling proteins by actin-stabilized endosomal microdomains. *Cell* **143**, 761–773 (2010).
26. B. Simonetti, P. J. Cullen, Actin-dependent endosomal receptor recycling. *Curr. Opin. Cell Biol.* **56**, 22–33 (2019).
27. O. L. Mooren, B. J. Galletta, J. A. Cooper, Roles for actin assembly in endocytosis. *Annu. Rev. Biochem.* **81**, 661–686 (2012).
28. E. D. Goley, M. D. Welch, The ARP2/3 complex: An actin nucleator comes of age. *Nat. Rev. Mol. Cell Biol.* **7**, 713–726 (2006).
29. D. Jia *et al.*, WASH and WAVE actin regulators of the Wiskott-Aldrich syndrome protein (WASP) family are controlled by analogous structurally related complexes. *Proc. Natl. Acad. Sci. U.S.A.* **107**, 10442–10447 (2010).
30. H. N. Higgs, T. D. Pollard, Regulation of actin polymerization by Arp2/3 complex and WASp/Scar proteins. *J. Biol. Chem.* **274**, 32531–32534 (1999).
31. M. M. Zaman *et al.*, Ubiquitination-deubiquitination by the TRIM27-USP7 complex regulates tumor necrosis factor alpha-induced apoptosis. *Mol. Cell Biol.* **33**, 4971–4984 (2013).
32. M. P. Peppelenbosch, L. G. Tertoolen, W. J. Hage, S. W. de Laat, Epidermal growth factor-induced actin remodeling is regulated by 5-lipoxygenase and cyclooxygenase products. *Cell* **74**, 565–575 (1993).
33. M. O. Aguilera, W. Beron, M. I. Colombo, The actin cytoskeleton participates in the early events of autophagosome formation upon starvation induced autophagy. *Autophagy* **8**, 1590–1603 (2012).
34. K. Yamada *et al.*, Small-molecule WNK inhibition regulates cardiovascular and renal function. *Nat. Chem. Biol.* **12**, 896–898 (2016).
35. A. Poswiata, K. Kozik, M. Miaczynska, D. Zdzalik-Bielecka, Endocytic trafficking of GAS6-AXL complexes is associated with sustained AKT activation. *Cell Mol. Life Sci.* **79**, 316 (2022).
36. C. Francavilla *et al.*, The binding of NCAM to FGFR1 induces a specific cellular response mediated by receptor trafficking. *J. Cell Biol.* **187**, 1101–1116 (2009).
37. A. Sato *et al.*, WNK regulates Wnt signalling and beta-Catenin levels by interfering with the interaction between beta-Catenin and GID. *Commun. Biol.* **3**, 666 (2020).
38. K. E. Longva *et al.*, Ubiquitination and proteasomal activity is required for transport of the EGF receptor to inner membranes of multivesicular bodies. *J. Cell Biol.* **156**, 843–854 (2002).
39. H. A. Alwan, E. J. van Zoelen, J. E. van Leeuwen, Ligand-induced lysosomal epidermal growth factor receptor (EGFR) degradation is preceded by proteasome-dependent EGFR de-ubiquitination. *J. Biol. Chem.* **278**, 35781–35790 (2003).
40. L. K. Goh, A. Sorkin, Endocytosis of receptor tyrosine kinases. *Cold Spring Harb. Perspect. Biol.* **5**, a017459 (2013).
41. M. Miaczynska, Effects of membrane trafficking on signaling by receptor tyrosine kinases. *Cold Spring Harb. Perspect. Biol.* **5**, a009035 (2013).
42. M. J. Crupi, D. S. Richardson, L. M. Mulligan, Cell surface biotinylation of receptor tyrosine kinases to investigate intracellular trafficking. *Methods Mol. Biol.* **1233**, 91–102 (2015).
43. A. Stanoev *et al.*, Interdependence between EGFR and phosphatases spatially established by vesicular dynamics generates a growth factor sensing and responding network. *Cell Syst.* **7**, 295–309.e11 (2018).
44. A. Simonsen *et al.*, EEA1 links PI(3)K function to Rab5 regulation of endosome fusion. *Nature* **394**, 494–498 (1998).
45. O. Ullrich, S. Reinsch, S. Urbe, M. Zerial, R. G. Parton, Rab11 regulates recycling through the pericentriolar recycling endosome. *J. Cell Biol.* **135**, 913–924 (1996).
46. E. Ohashi *et al.*, Receptor sorting within endosomal trafficking pathway is facilitated by dynamic actin filaments. *PLoS One* **6**, e19942 (2011).
47. L. Sun, Z. J. Chen, The novel functions of ubiquitination in signaling. *Curr. Opin. Cell Biol.* **16**, 119–126 (2004).
48. J. Taunton *et al.*, Actin-dependent propulsion of endosomes and lysosomes by recruitment of N-WASP. *J. Cell Biol.* **148**, 519–530 (2000).
49. S. Zhuang, G. D. Ouedraogo, I. E. Kochevar, Downregulation of epidermal growth factor receptor signaling by singlet oxygen through activation of caspase-3 and protein phosphatases. *Oncogene* **22**, 4413–4424 (2003).
50. M. Chen, L. M. Chen, C. Y. Lin, K. X. Chai, The epidermal growth factor receptor (EGFR) is proteolytically modified by the Matriptase-Prostasin serine protease cascade in cultured epithelial cells. *Biochim. Biophys. Acta* **1783**, 896–903 (2008).
51. M. Higuchi, K. Onishi, C. Kikuchi, Y. Gotoh, Scaffolding function of PAK in the PDK1-Akt pathway. *Nat. Cell Biol.* **10**, 1356–1364 (2008).
52. S. Maddika, J. Chen, Protein kinase DYRK2 is a scaffold that facilitates assembly of an E3 ligase. *Nat. Cell Biol.* **11**, 409–419 (2009).
53. T. Pleiner *et al.*, WNK1 is an assembly factor for the human ER membrane protein complex. *Mol. Cell* **81**, 2693–2704.e12 (2021).
54. M. Vouri *et al.*, Axl-EGFR receptor tyrosine kinase hetero-interaction provides EGFR with access to pro-invasive signalling in cancer cells. *Oncogenesis* **5**, e266 (2016).
55. X. Shao, Q. Li, A. Mogilner, A. D. Bershadsky, G. V. Shivashankar, Mechanical stimulation induces formin-dependent assembly of a perinuclear actin rim. *Proc. Natl. Acad. Sci. U.S.A.* **112**, E2595–E2601 (2015).
56. J. Kim, M. Kundu, B. Viollet, K. L. Guan, AMPK and mTOR regulate autophagy through direct phosphorylation of Ulk1. *Nat. Cell Biol.* **13**, 132–141 (2011).
57. Y. Yang *et al.*, TRIM27 cooperates with STK38L to inhibit ULK1-mediated autophagy and promote tumorigenesis. *EMBO J.* **41**, e109777 (2022).
58. J. B. Casaletto, A. I. McClatchey, Spatial regulation of receptor tyrosine kinases in development and cancer. *Nat. Rev. Cancer* **12**, 387–400 (2012).
59. G. Zoumpoulidou *et al.*, Role of the tripartite motif protein 27 in cancer development. *J. Natl. Cancer Inst.* **104**, 941–952 (2012).
60. Z. A. Gibbs *et al.*, The testis protein ZNF165 is a SMAD3 cofactor that coordinates oncogenic TGFbeta signaling in triple-negative breast cancer. *Elife* **9**, e57679 (2020).
61. J. U. Jung, A. B. Jaykumar, M. H. Cobb, WNK1 in malignant behaviors: A potential target for cancer? *Front. Cell Dev. Biol.* **10**, 935318 (2022).
62. H. A. Dbouk *et al.*, Actions of the protein kinase WNK1 on endothelial cells are differentially mediated by its substrate kinases OSR1 and SPAK. *Proc. Natl. Acad. Sci. U.S.A.* **111**, 15999–16004 (2014).